Journal of Catalysis 285 (2012) 168–176

Contents lists available at SciVerse ScienceDirect

Journal of Catalysis

journal homepage: www.elsevier.com/locate/jcat

Epoxidation catalysts derived from introduction of titanium centers onto the surface of mesoporous aluminophosphate: Comparisons with analogous catalysts based on mesoporous silica

Lorraine Raboin [a,b,1], Junko Yano [c], T. Don Tilley [a,b,*]

[a] Department of Chemistry, University of California, Berkeley, CA 94720-1461, USA
[b] Chemical Sciences Division, Lawrence Berkeley National Laboratory, 1 Cyclotron Road, Berkeley, CA 94720, USA
[c] Physical Biosciences Division, Lawrence Berkeley National Laboratory, 1 Cyclotron Road, Berkeley, CA 94720, USA

ARTICLE INFO

Article history:
Received 26 July 2011
Revised 15 September 2011
Accepted 22 September 2011
Available online 26 October 2011

Keywords:
Mesoporous aluminophosphates
Titanium isopropoxide
Ti-grafted aluminophosphates
Ti-grafted SBA-15
Cyclohexene catalytic oxidation

ABSTRACT

Titanium/AlPO materials were prepared by grafting a titanium alkoxide (titanium isopropoxide) onto a mesoporous aluminophosphate. The structures of the surface-bound titanium species were investigated by UV–vis, FTIR, MAS NMR, and XANES/EXAFS spectroscopies. The titanium anchoring occurs by reaction between the alkoxide precursor and surface Al–OH and P–OH groups of the AlPO support. The titanium species exist in isolated tetrahedral coordination environments, and as oligomerized species. The catalysts prepared are selective and active for the liquid-phase epoxidation of cyclohexene in the presence of TBHP. The observed activities and selectivities were comparable with those obtained for similarly prepared titanium/SBA-15 samples of similar Ti content (but higher BET surface area).

Published by Elsevier Inc.

1. Introduction

Heterogeneous catalytic oxidation processes play an important role in the chemical industry [1]. Among the oxidation catalysts that have attracted strong interest are titanium-containing silicate and aluminosilicate materials (e.g., TS-1, TS-2, Ti-ß, and Ti-ZMS), which have been shown to be effective in selective oxidations such as olefin epoxidation [2–4] and alkane conversions to alcohols and ketones [4–6]. Since the introduction of M41S materials in 1992 [7], considerable attention has additionally focused on mesoporous, titanium-containing catalysts. Thus, mesoporous titanium–silica catalysts such as Ti-MCM-41 and Ti-SBA-15, with much larger pore sizes, have been extensively investigated for epoxidations of a range of olefins [8–10]. Attractive features of such catalysts include their regular pore structures, their large pore sizes, and their high surface areas. The large pores of these materials readily allow chemical modifications of the catalyst surface and utilization of large molecular substrates.

Aluminophosphate (AlPO) materials, composed of tetrahedral AlO_4^- and PO_4^+ units that form electroneutral frameworks, represent the first examples of inorganic molecular sieves composed of oxides other than silicates or aluminosilicates [11]. Since their discovery, various aluminophosphate-based molecular sieves, including mesoporous structures, have been reported [12–14]. Interest in these materials as catalysts or catalyst supports developed rapidly with the realization that other ions could be incorporated into the aluminophosphate framework. It has proven possible to incorporate various transition metals ions, via substitution of Al and/or P atoms, to give metal-containing aluminophosphates. Such materials have been extensively investigated with respect to catalytic applications [15–18].

Titanium cations may be incorporated into the framework of aluminophosphates, by substitution into P(V) sites, to give tetrahedral Ti(IV) sites with catalytic properties that are distinct from those of other titanium-based materials. Titanium-containing microporous aluminophosphates, such as Ti-AlPO-5 [19–21], Ti-AlPO-11 [19,20], and Ti-AlPO-VPI5 [21,22], have been extensively studied along with their catalytic performances for oxidations. In addition, Ti-substituted hexagonal mesoporous aluminophosphate (Ti-HMA) materials exhibit promising catalytic properties for selective oxidations of cycloalkanes [23], phenols [24], and olefins [25]. Interestingly, these catalysts are better than analogous, mesoporous, titanium-substituted silicas (Ti-MCM-41) for the oxidation of phenols [24], and the epoxidation of olefins [25].

* Corresponding author at: Department of Chemistry, University of California, Berkeley, CA 94720-1461, USA. Fax: +1 510 642 8940.
E-mail addresses: lraboin@chem.ucla.edu (L. Raboin), jyano@lbl.gov (J. Yano), tdtilley@berkeley.edu (T.D. Tilley).
[1] Present address: University of California, Los Angeles, Department of Chemistry and Biochemistry, Los Angeles, CA 90095, USA.

0021-9517/$ - see front matter Published by Elsevier Inc.
doi:10.1016/j.jcat.2011.09.023

The inner walls of mesoporous AlPOs possess exposed hydroxyls groups (Al–OH and P–OH) that may be used for surface modification and the introduction of catalytic centers via grafting reactions. This contribution describes the use of mesoporous AlPO as a support for catalytic titanium centers, introduced by a chemical grafting method with use of molecular precursors. While framework-substituted Ti-AlPOs have been studied as catalysts, the chemically directed introduction of titanium centers onto the surface of mesoporous AlPOs has not received much attention. Gianotti et al. [26] described the introduction of surface, tetrahedral titanium species via reaction of titanocene dichloride, Cp_2TiCl_2, with a mesoporous AlPO, to produce a material that exhibited mildly Brønsted acidic properties. However, the catalytic properties of this material have not been reported.

In this paper, we report the behavior of a mesoporous aluminophosphate prepared under non-aqueous conditions starting from inorganic precursors [27,28]. Titanium centers were introduced onto the surface by use of titanium isopropoxide, $Ti(O^iPr)_4$, as a molecular precursor. The new Ti-AlPO material has been investigated as a catalyst for the oxidation of cyclohexene in the presence of *tert*-butyl hydroperoxide (TBHP) or hydrogen peroxide (H_2O_2). These results are compared with those obtained with a similar catalyst prepared with mesoporous silica SBA-15 as the support. The structural nature of the titanium centers on the Ti-AlPO material was probed with a variety of characterization methods, including infrared, DRUV–vis, NMR, and X-ray absorption spectroscopies.

2. Material and methods

2.1. General procedures

All manipulations were performed under an atmosphere of nitrogen with standard Schlenk techniques and/or a Vacuum Atmospheres drybox. Dry, oxygen-free solvents were used throughout. All reagents were purchased from Aldrich except triblock copolymer Pluronic F127 ($EO_{106}PO_{70}EO_{106}$), which was purchased from BASF and used as received. Cyclohexene was distilled prior to use. Mesoporous SBA-15 silica was synthesized according to a literature procedure [29].

2.2. Synthesis of AlPO

Mesoporous aluminophosphate (AlPO) was synthesized following the procedure established in the literature [28]. In a typical reaction, 5 mmol of $AlCl_3$, 5 mmol of H_3PO_4 and 0.1 mmol of F127 were added to 0.65 mol of ethanol. The mixture was stirred vigorously for 30 min at room temperature and transferred into a beaker for evaporation of the ethanol at 40 °C for 6 h and then at 80 °C for an additional 2 h. The as-synthesized products were calcined at 550 °C for 6 h in a flow of O_2 to remove the template.

2.3. Grafting of $Ti(O^iPr)_4$

To avoid the presence of physisorbed water before the grafting procedure, the supports (AlPO and SBA-15) were dehydrated at 130 °C for 24 h under a dynamic vacuum and thereafter handled under a nitrogen atmosphere. A 0.5-g sample of the support was suspended in hexane (25 mL). A hexane solution (30 mL) of the titanium precursor $Ti(O^iPr)_4$ was prepared and added to the suspended support via a cannula. The precursor was added in large excess on the basis of the number of surface hydroxyl groups present on the support (molar ratio Ti:OH = 5:1). The resulting suspension was stirred at room temperature for 25 h and then filtered and washed with hexane (3 × 25 mL). The grafted material was dried at room temperature under vacuum and stored in a drybox. The resulting samples are referred to as Ti-AlPO and Ti-SBA15.

Additional samples were prepared by calcination of the initially grafted materials at 300 °C (5 °C min^{-1}) for 3 h in a flow of O_2. This treatment provided samples designated as Ti-AlPOC and Ti-SBA15C. Calcinations were performed using a Lindberg 1200 °C three-zone tube furnace.

2.4. Preparation of surface-modified Me_{cap}Ti-AlPO

An additional catalyst was prepared by modification of the calcined Ti-AlPO material according to the procedure developed by Brutchey et al., and described in [9]. A 0.250-g sample of the unmodified Ti-AlPOC catalyst was suspended in 20 mL of hexane. A 10 mL solution of $Me_3Si(NMe_2)$ in hexane (five equiv based on surface hydroxyl content) was added via a cannula at room temperature. The suspension was stirred for 20 h at room temperature under flowing nitrogen. The solid was then filtered on a Büchner funnel and rinsed with hexane (3 × 10 mL). The resulting solid was dried at 130 °C under vacuum for 24 h and stored in a drybox.

2.5. Catalysis procedure

A sample of the catalyst (ca. 0.025 g) was added to a 50-mL round-bottom flask that was fitted with a reflux condenser and a septum. Dry acetonitrile (5.0 mL) and distilled cyclohexene (1.00 mL) were added by syringe through the septum under a flow of nitrogen. Dodecane (0.100 mL) was added as an internal standard via micropipette. The mixture was allowed to equilibrate at the reaction temperature of 65 °C for 10 min. *Tert*-butyl hydroperoxide TBHP (5 M in decane – 1.1 mL) or hydrogen peroxide H_2O_2 (30 wt.% in H_2O – 0.62 mL) was added by syringe to the rapidly stirred solution. Aliquots (ca. 0.1 mL) were removed from the reaction mixture by syringe after 0.5, 1, 2, 4, 6, and 24 h, and then filtered. The filtrate was analyzed by gas chromatography (GC), and the assignments were made by comparison with authentic samples analyzed under the same conditions.

2.6. Characterization

N_2 adsorption–desorption isotherms were measured on a Quantachrome Autosorb 1 analyzer with all samples heated at 120 °C under vacuum for 20 h prior to data collection. Surface area and pore volume analyses were calculated according to the Brunauer–Emmett–Teller (BET) method, and the pore size distributions were obtained based on the adsorption branch of the isotherm with the Barrett–Joyner–Halenda (BJH) method. DRUV–vis spectra were recorded on a Varian Cary 300 UV–vis spectrometer with MgO as a reference. *In situ* FTIR measurements were acquired on a Nicolet 6700 spectrometer by mounting a self-sustaining pellet of the sample in an airtight cell equipped with KCl windows, in which the sample was dehydrated under vacuum for 1 h at 180 °C before measurements. For solid-state NMR experiments, the samples were transferred in the drybox into a 4 mm MAS rotor. ^1H, ^{13}C, ^{27}Al, ^{29}Si, and ^{31}P MAS NMR spectra were collected at room temperature on a Bruker Avance-500 spectrometer operating at resonance frequencies of 500.23, 125.78, 130.34, 99.38, and 202.50 MHz, respectively. The MAS rotor spinning was in a range of 9–11 kHz. The chemical shifts of ^{27}Al, ^{29}Si, and ^{31}P were calibrated according to 1 M $Al(NO_3)_3$ solution, polydimethylsiloxane (PDMS), and 85% H_3PO_4 solution, respectively. The ^{13}C CP/MAS (cross polarization/magic angle spinning) NMR spectra were collected using a 4.2 μs 90° proton pulse with a contact time of 2 ms and a relaxation delay of 2 s. X-ray Absorption Spectroscopy (XANES and EXAFS) measurements were taken at the Stanford Synchrotron Radiation Lightsource (SSRL) and at the

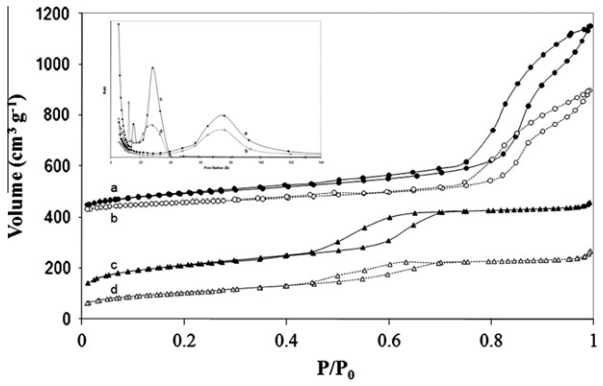

Fig. 1. Nitrogen adsorption–desorption isotherms for (a) mesoporous AlPO, (b) Ti-AlPO, (c) SBA15, and (d) Ti-SBA15. Curves (a) and (b) have been moved up by 400 $cm^3\ g^{-1}$. Pore size distributions calculated from the adsorption isotherm branch are shown as insets.

Advanced Light Source (ALS) in Berkeley. Ti K-edge absorption measurements were taken at SSRL on beamline 4–3 at an electron energy of 3.0 GeV with an average current of 90 mA and at the ALS on beamline 10.3.2 at an electron energy of 1.9 GeV with an average current of 500 mA. Both beamlines were equipped with a Si(1 1 1) double-crystal monochromator, and its energy calibration (4966.0 eV) was checked at the rising edge of Ti foil. Spectra were measured as fluorescence excitation spectra. Samples were packed in a Ti-free Mylar tape, and the data were collected at cryogenic temperature (~50 K) using a liquid helium cryosteam (at SSRL) and at room temperature (at ALS). GC analyses were performed with an HP 6890 GC system using a methylsiloxane capillary column (50.0 × 320 × 1.05 μm nominal), and integration was performed relative to an internal standard (dodecane). Elemental analyses (ICP–AES) were performed by Galbraith Laboratories.

3. Results and discussion

3.1. Synthesis and characterization of the supports

The mesoporous silica SBA-15 [29] and mesoporous aluminophosphate AlPO [28] materials were synthesized according to procedures in the literature. Mesoporous AlPO was prepared by using the block copolymer Pluronic F127 ($EO_{106}PO_{70}EO_{106}$) as a structure-directing agent with $AlCl_3/H_3PO_4$ as the inorganic precursors. Nitrogen adsorption–desorption measurements confirmed the mesoporous structures of both calcined supports, as these materials exhibit the expected type IV isotherms (Fig. 1). Mesoporous SBA-15 silica exhibits a H1 hysteresis loop that is characteristic of channels with uniform sizes and shapes. In the case of the AlPO sample, the observed hysteresis resembles an H3-type hysteresis, which indicates a distribution of pore sizes (Fi. 1, inset). The sharp inflexion characteristic of capillary condensation within the mesopores appears at a higher partial pressure for the AlPO material (at $P/P_0 \sim 0.9$; vs. $P/P_0 \sim 0.6$ for SBA-15), suggesting larger pore sizes as is expected with the use of Pluronic F127 as a template. Indeed, the calculated pore sizes of the AlPO and SBA-15 samples are 15.1 and 5.60 nm, and the BET surface areas are 329 and 686 $m^2\ g^{-1}$, respectively (Table 1).

The mesoporous AlPO was also characterized by ^{27}Al and ^{31}P MAS NMR spectroscopy (refer to Fig. A1). These results revealed that after calcination, the framework is mainly composed of alternating $(AlO_4)^-$ and $(PO_4)^+$ tetrahedra, suggestive of a highly condensed framework. In addition, the ^{31}P NMR spectrum exhibited a broad peak at > 0 ppm, previously ascribed to the presence of isolated PO_4 units (i.e., PO_4^{3-}, HPO_4^{2-}, H_2PO^{4-}, or H_3PO_4) [30]. The presence of such species has been attributed to the non-aqueous conditions used for the AlPO synthesis, which tends to decrease the degree of dissociation of H_3PO_4 in solution and thus their condensation with Al species [31]. This hypothesis is in good agreement with a Al/P molar ratio found to be somewhat less than 1 (0.9), as determined by elemental analysis.

The concentration of OH sites on the surface of the supports was determined by monitoring reactions of the materials with $Mg(CH_2Ph)_2{\cdot}2THF$ and quantifying the amount of toluene evolved after the reaction by ^1H NMR spectroscopy [9,32]. By this method, the OH density on the surface of AlPO was determined to be 3.78 ± 0.4 OH/nm^2. To our knowledge, the OH coverage of this AlPO material has not been previously reported. These hydroxyl groups may exist as both Al–OH and P–OH sites that line the inner surface of the pores. This relatively high value is in agreement with the presence of incompletely reacted H_3PO_4 (as observed by solid-state NMR), as such species contain extra-framework terminal P–O bonds (P═O and/or P–OH). For comparison, the concentration of OH sites on SBA-15 was determined to be 1.63 ± 0.2 OH/nm^2, which is in the range of previously reported values [10,32].

3.2. Grafting of the titanium precursor

The titanium isopropoxide precursor $Ti(O^iPr)_4$ was grafted by stirring a suspension of the support in a hexane solution of the precursor for 25 h at room temperature. An excess of the precursor was used to ensure a total coverage of the surface. For both supports, the pore diameter is much larger than the estimated size of the precursor (radius of ca. 4.4 Å [33]), which permits diffusion of the precursors molecules into the channels, thus leading to maximum titanium loadings of 2.57 and 5.32 wt.% for AlPO and SBA-15, respectively, as determined by elemental analysis performed on uncalcined Ti-grafted materials (Table 1). These values were reproducible within an error ca. 10%. The maximum surface coverage (ca. 0.98 Ti/nm^{-2}) does not vary according to the nature of the support even though the number of initial surface hydroxyl groups for AlPO (ca. 3.78 OH/nm^{-2}) is twice that of SBA-15 (ca. 1.63 OH/nm^{-2}). This suggests that both surfaces are saturated with titanium species upon grafting. In addition, a higher amount of residual OH groups at the surface of AlPO is expected after grafting of $Ti(O^iPr)_4$, in comparison with SBA-15. The value for the titanium coverage on SBA-15 is in agreement with a value previously reported by Jarupatrakorn et al. (complete coverage of 1.06 Ti/nm^{-2}) [10].

Nitrogen porosimetry was used to evaluate the pore morphologies and surface areas of the uncalcined Ti-AlPO and Ti-SBA-15 materials obtained. The isotherms for the titanium-containing materials exhibit type IV behavior (Fig. 1), which means that the mesoporous structures are maintained after grafting. As expected,

Table 1
Physicochemical properties of supports and Ti-grafted samples.

Sample	Ti loading (wt.%)	Ti loading (Ti/nm^{-2})	BET surface area ($m^2\ g^{-1}$)	Pore volume ($cm^3\ g^{-1}$)	Pore diameter (nm)
AlPO	–	–	329	1.07	15.1
Ti-AlPO	2.57	0.98	213	0.7	15.1
SBA15	–	–	686	0.69	5.60
Ti-SBA15	5.32	0.98	363	0.37	5.60

both the surface area and the pore volume decrease upon addition of the titanium species (Table 1). The high decreases are in good agreement with previous studies on grafting of SBA-15 by an excess of $Ti(O^iPr)_4$ [10,34]. However, as an excess of $Ti(O^iPr)_4$ was used, the high reduction of the surface area may be interpreted as a possible pore blocking upon the grafting of the titanium species.

In situ infrared spectroscopy was used to study the behavior of the surface hydroxyls throughout the grafting process. Prior to analysis, the samples were heated at 180 °C under vacuum for 1 h to remove physisorbed water. Fig. 2 shows FTIR spectra in the OH stretching region for pure mesoporous AlPO (curve a), uncalcined Ti-grafted AlPO (curve b), pure silica SBA-15 (curve c), and uncalcined Ti-grafted SBA-15 (curve d). The AlPO spectrum (curve a) exhibits one main absorption band at 3680 cm^{-1}, attributable to the stretching mode for isolated P-OH groups [26,35]. These groups may be present as terminal P-OH groups on the external surface of the channels, as defects present in the structure and/or as extra-framework terminal P–OH groups of incompletely condensed species. The spectrum also shows a band of low intensity at 3790 cm^{-1} due to the stretching mode for Al–OH groups of Al in tetrahedral coordination [26,36]. Similar bands are present in the Ti-AlPO spectrum after grafting (curve b), with a lower intensity for the main P–OH absorption. This indicates that the titanium precursors graft by reaction with the P–OH groups and that residual, unreacted P–OH groups are still present after the grafting. The presence of residual hydroxyl groups is in agreement with the amount of initial surface hydroxyl groups (ca. 3.78 OH/nm^{-2}) compared with the amount of grafted titanium species (ca. 0.98 Ti/nm^{-2}). However, due to the initial poor intensity of the characteristic band for Al–OH, it is not possible to draw conclusions concerning their role in the grafting of titanium isoproxide. For the SBA-15 support, the spectrum exhibits a unique sharp band at 3740 cm^{-1}, before grafting, attributed to the stretching vibration of isolated silanol groups located at the surface of the internal walls of the silica channels. The intensity of the Si–OH band is completely diminished after introduction of the excess of $Ti(O^iPr)_4$, indicating their extensive participation in the grafting process. A shoulder at ca. 3720 cm^{-1} is present after grafting. This band may be attributed to Brønsted acidic OH groups interacting with Ti sites [37]. At the same time, for both AlPO and SBA-15 supports, new bands appear after grafting in the C–H region (3100–2800 cm^{-1}), assigned to 2-propoxide ligand vibrations [38].

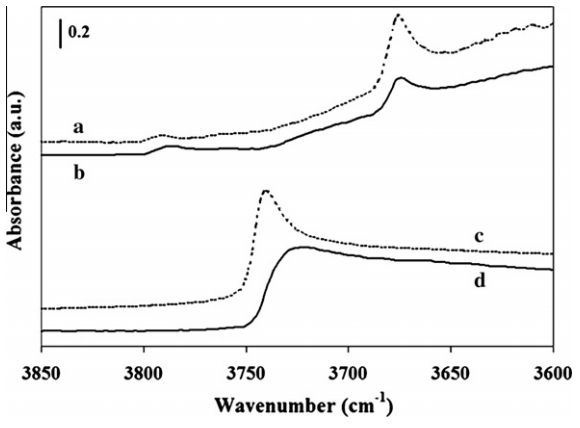

Fig. 2. In situ FTIR spectra of (a) calcined mesoporous AlPO, (b) Ti-AlPO, (c) SBA-15 and (d) Ti-SBA15. The spectrum for Ti-AlPO material is obtained after normalizing the region in the range of 2000–2600 cm^{-1} assigned to the overtone modes of Al–O–P, and the spectrum for Ti-SBA15 materials is obtained after normalizing the peak intensity at the 1990 cm^{-1} band assigned to the overtone mode of silica framework.

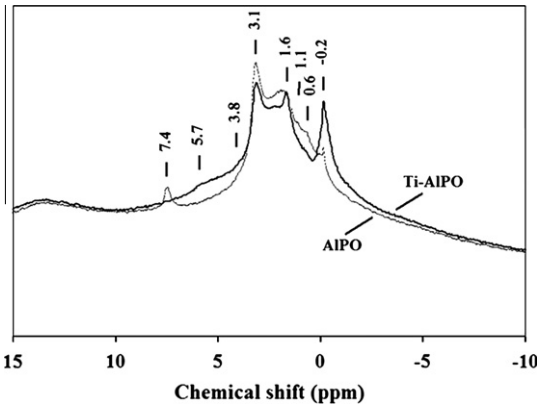

Fig. 3. ^1H MAS NMR spectra of dehydrated AlPO (dot line) and Ti-AlPO (solid line) samples. Spin rate, 9 kHz.

To gain further information on the nature of the hydroxyls groups involved in the grafting of $Ti(O^iPr)_4$ onto AlPO, a study by ^1H MAS NMR spectroscopy was conducted. The spectra, shown in Fig. 3, were acquired for AlPO and uncalcined Ti-AlPO samples dehydrated at 130 °C under vacuum for 24 h. The AlPO spectrum exhibits peaks extending from −0.2 to 3.2 ppm with an additional peak at 7.4 ppm. According to the previous reports [39,40], the peaks observed in the 0.6–1.4 ppm region are probably due to non-acidic terminal Al-OH groups, while the peak at 1.7 ppm is generally assigned to terminal P-OH groups, and this is consistent with results from infrared spectroscopy. The signal at 3.1 ppm is in the range of signals observed for the formation of hydrogen bonds between the Al–OH groups at extra-framework aluminum species and neighboring oxygen atoms, in zeolites [41–43] or AlPOs [40]. The signals in the range of 8–11 ppm have previously been observed for AlPO materials prepared with Al/P ratios less than 1 [44] and in the study of partly condensed BFO_4 [45]. These signals were assigned to the existence of Al or B sites bonded to incompletely reacted phosphoric acid. We believe that the signal observed at 7.5 ppm corresponds to such species, which would confirm the observations obtained by ^{31}P MAS NMR spectroscopy (*vide supra*). After treatment with $Ti(O^iPr)_4$, this peak completely disappeared, indicating that the precursors preferentially react with the most acidic protons of the P–OH groups of these partially condensed H_3PO_4 species. In addition, a decrease in the signals assigned to terminal Al–OH groups (0.6–1.4 ppm) was observed, indicating that the titanium isopropoxide grafts to both acidic Al–OH and P–OH groups. After grafting, a broad signal composed of several peaks from 3.8 to 6.0 ppm appeared. By analogy with observations previously reported for SAPO materials [39,46], we ascribe these signals to the presence of bridging hydroxyl groups in Ti–(OH)–M linkages, where M is Al or P, and/or to water interacting with acid sites of Ti–(OH)–M. Finally, the appearance of a strong signal at −0.2 ppm was assigned to methyl CH_3 groups of $Ti(O^iPr)$ species.

3.3. Characterization of the grafted titanium centers

DRUV–vis spectroscopy is a sensitive tool to probe the local environment of the titanium atoms at the surface of the grafted materials. The spectra for Ti-AlPO and Ti-SBA15 samples are given in Fig. 4. Before calcination at 300 °C under a flow of O_2 (Fig. 4a), a band centered at ca. 216 nm is observed for both materials. Such an absorption, with a maximum at about 200–220 nm, is characteristic of the ligand-to-metal charge transfer (LMCT) involving isolated Ti(IV) atoms in tetrahedral coordination [47–49]. In addition, a shoulder at ca. 255 nm is present for both Ti-AlPO and Ti-SBA15,

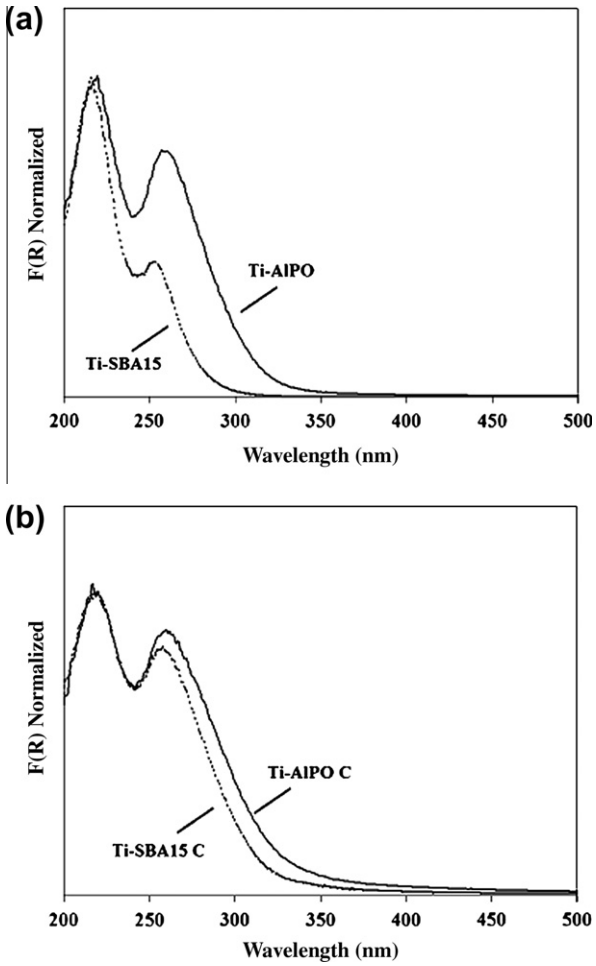

Fig. 4. DRUV–vis spectra of Ti-AlPO and Ti-SBA15 samples (a) uncalcined and (b) calcined at 300 °C for 3 h under a flow of O_2.

which suggests the presence of some oligomeric species and/or TiO_2-like nanoclusters [48,49]. This behavior can be related to the use of titanium isopropoxide, which is very reactive and known to form oligomeric titano-oxo species [50,51]. Furthermore, the band at 255 nm may be ascribed to the presence of Ti–O–Ti dimeric structures. This hypothesis is supported by a previously reported UV spectrum [52] for a dimeric titanium compound (a titanosilsesquioxane) in which Ti(IV) ions are linked by oxygen bridges. This compound exhibits a major absorption at around 240 nm. No other spectral features are present, and the absence of a band at about 330 nm indicates that titania particles (anatase) are not present in the materials. By comparing the shapes of the absorption bands for Ti-AlPO and Ti-SBA15, we conclude that the Ti local environment is similar for these materials and does not noticeably depend on the nature of the support: the titanium species exist in isolated tetrahedral coordination environments and as oligomerized – possibly dimeric – species. However, the band at about 255 nm is more intense for Ti-AlPO than for Ti-SBA15, which may indicate a somewhat more important contribution of oligomerized species at the surface of AlPO. The DRUV–vis spectra for calcined materials are similar to those for the uncalcined materials, suggesting only a slight change in the Ti coordination environment upon calcination (Fig. 4b). The bands for the calcined materials are broader, indicating a broader distribution of Ti environments. Small shifts in the λ_{max} values are also observed upon calcination (ca. 3 nm), which is consistent with small changes in the coordination environment of titanium species (e.g., $Ti(OH)(OM)_3$ to $Ti(OM)_4$, where M = Si, Al or P).

The grafting process was also studied by ^{13}C solid state NMR spectroscopy. The ^{13}C CP/MAS spectra of uncalcined Ti-grafted AlPO and Ti-grafted SBA15 samples (Fig. 5a and Fig. 5b) are similar and consist of three resonances at about 24, 66, and 80 ppm. The resonances at 24 and 80 ppm have been previously observed for $Ti(O^iPr)_4$-grafted silica materials [50,53] and are assigned to methyl and methine carbons of the isopropyl groups, respectively. For comparison, the spectrum of $Ti(O^iPr)_4$ in solution exhibits resonances at 26.6 and 76.2 ppm in $CDCl_3$. The additional peak at 66 ppm may be assigned to the presence of bridging isopropoxide groups ($Ti(\mu\text{-}O^iPr)Ti$) [54].

Titanium K-edge XANES is a complementary characterization tool that offers a powerful method for probing titanium coordination environments. The pre-edge peak position and intensity are sensitive to the symmetry of the donor atoms in the coordination sphere and permit assignment of coordination numbers. Indeed, the pre-edge peak energy is expected to be low and the intensity high in non-centrosymmetric environments (i.e., tetrahedral), whereas in symmetrical environments (i.e., octahedral), the opposite is observed [55,56]. Fig. 6 shows Ti K-edge XANES spectra of uncalcined Ti-AlPO and Ti-SBA15. Both spectra exhibit a weak, broad pre-edge feature at photon energy of around 4969 eV, which could suggest the presence of grafted titanium atoms in octahedral coordination. The Ti-SBA15 sample exhibits a pre-edge peak that is less well resolved than that for the Ti-AlPO sample with a slightly lower intensity. This indicates a higher average coordination number for the titanium atoms of Ti-SBA15. To better estimate the coordination number of the Ti atoms, the pre-edge peak intensities were plotted against the peak positions and compared with

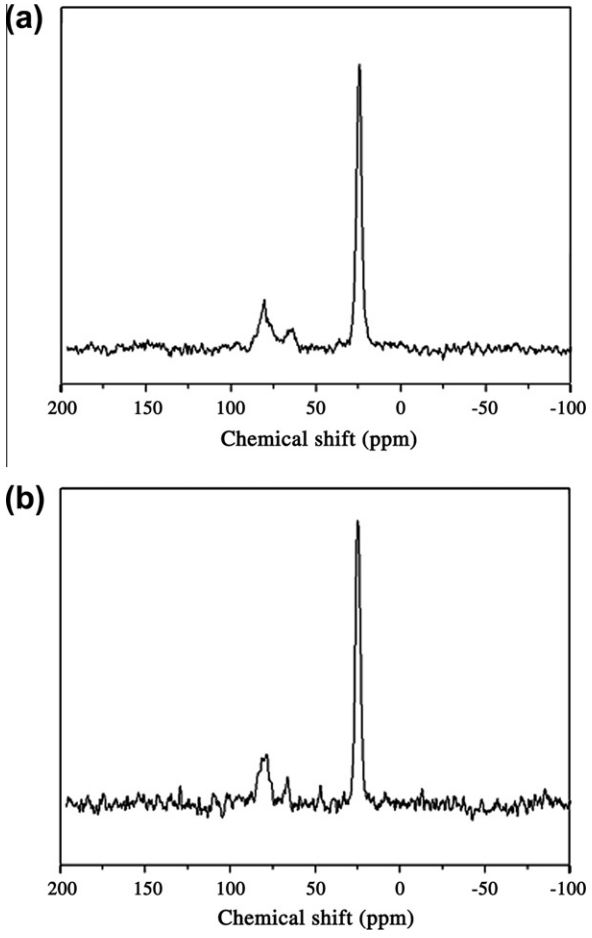

Fig. 5. ^{13}C CP/MAS spectra of $Ti(O^iPr)_4$ grafted on (a) mesoporous AlPO or (b) SBA-15.

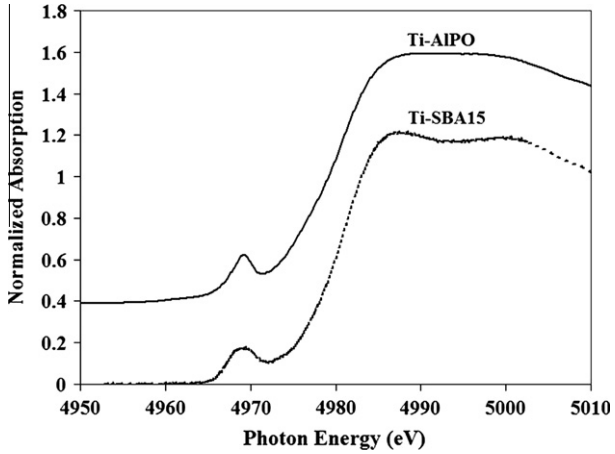

Fig. 6. Ti K-edge XANES spectra of uncalcined Ti-AlPO and Ti-SBA15. The spectrum for the Ti-AlPO sample is offset vertically for clarity.

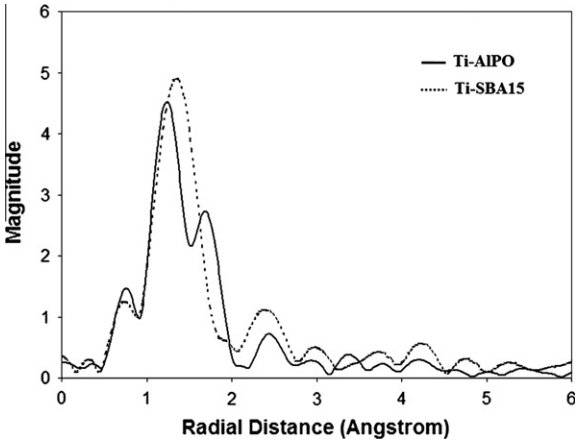

Fig. 8. Ti K-edge EXAFS Fourier transforms of uncalcined Ti-AlPO and Ti-SBA15 (not corrected for phase shift).

corresponding values for literature Ti compounds (Fig. 7) [57]. Farges et al. [57] found three well-defined domains for Ti reference compounds that are defined by the Ti coordination geometry: the upper left region corresponds to 4-coordinate Ti (e.g., Ba_2TiO_4), while the lower right region contains 6-coordinate Ti species (e.g., anatase). The middle region corresponds to 5-coordinate titanium (e.g., fresnoite). The Ti-grafted AlPO and silica materials do not belong to one of these regions, but fall in an area defined by a lower peak intensity and position. Similar observations have been previously obtained for titanium grafted on mesoporous MCM-41 [58,59] or various others silicas [51,60] and suggest a mixture of Ti coordination environments. For both samples, the peak position belongs to an energy corresponding to 4-coordinate Ti sites, but these peaks have a low intensity that likely reflects the presence of higher coordination numbers. The coordination of Ti is increased up to six because of the presence of oligomerized species and/or the hydratation of the samples [61].

FT-EXAFS data for the Ti-AlPO and Ti-SBA15 samples were also analyzed to get further information about the coordination environment of Ti. The results are shown on Fig. 8. The spectra show a maximum for the first peak, corresponding to the first shell Ti–O, of 1.76 ± 0.02 and 1.84 ± 0.02 Å, for Ti-AlPO and Ti-SBA15, respectively. This indicates a predominantly fourfold coordination geometry by comparing with reported average Ti–O distances of 1.81 Å in the tetrahedrally coordinated Ti model compound Ba_2TiO_4 [62], 1.92 Å for pentacoordinated Ti (fresnoite) [63], and about 1.94–2.02 Å for sixfold coordination [64]. The longer averaged Ti–O distance for the Ti-SBA15 sample suggests that the amount of titanium in the higher coordination state increases in comparison with the Ti-AlPO sample, in agreement with the XANES results.

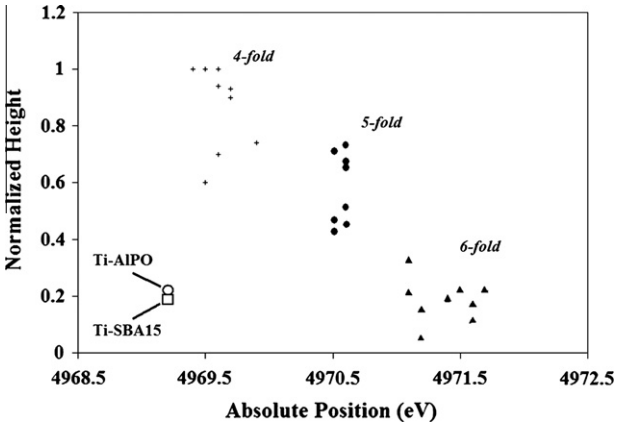

Fig. 7. Comparison of the pre-edge energies and heights of uncalcined Ti-AlPO and Ti-SBA15 with reference compounds taken from the literature [57].

3.4. Catalytic oxidation of cyclohexene

Catalytic studies were undertaken to compare inherent activities and selectivities associated with titanium catalysts on the two types of support – mesoporous silica and aluminophosphate. All the heterogeneous catalysts were tested in the epoxidation of cyclohexene with *tert*-butyl hydroperoxide (TBHP) as an oxidant at 65 °C in acetonitrile. In Table 2, the results of cyclohexene oxidation using Ti-AlPO, Ti-AlPOC, Ti-SBA15, and Ti-SBA15C are depicted (C denotes the samples calcined at 300 °C/O_2/3 h). Selectivities and total yields (moles of cyclohexene oxide products relative to initial TBHP concentration) after a reaction time of 6 h are given for the main products, as determined by gas chromatography (GC) analysis. These products are cyclohexene epoxide (epoxide), cyclohexan-1,2-diol (diol), 2-cyclohexen-1-ol (ene-ol) and 2-cyclohexen-1-one (ene-one). For longer reaction times (>6 h), very little further conversion to products was observed.

The uncalcined Ti-AlPO material was found to be active for the oxidation of cyclohexene, exhibiting a total yield of 6.2% (epoxide selectivity 93%), and a turnover number, TON (moles of epoxide per moles of Ti), of 24. Although examples of framework-substituted Ti-AlPOs have been reported to be active for the oxidation of cyclohexene (in the presence of H_2O_2) [65–67], the results presented here represent the first evidence that mesoporous AlPO as a support for titanium centers, introduced by a chemical grafting, exhibit a catalytic activity. In addition, the Ti-AlPO and Ti-SBA15 catalysts exhibit similar catalytic properties (Table 2). The activity of Ti-AlPO is found to be only slightly below that of Ti-SBA15, as the Ti-SBA15 material shows a total yield of 16% (epoxide selectivity > 99%) and a TON of 30. To make comparisons between the systems investigated in this study and those reported in the literature, the activities were expressed as turnover frequencies (TOFs, defined as moles of epoxide formed per mole of titanium after 1 h of reaction, in Table 2). TOF values were determined to be in the range of 15–20 h^{-1} for the uncalcined catalysts, with similar titanium coverages (ca. 1.0 Ti/nm^{-2}). These values are in the same range as those reported for the production of cyclohexene epoxide (from TBHP oxidant) by catalysts prepared by introduction of Ti using an excess of $Ti(O^iPr)_4$ onto a MCM-41 surface (TOF = 14 at 25 °C [68]) or onto aerosil silica (TOF = 10 at RT [69]). In these cases, the selectivities for epoxidation were also high (90% after 1 h [68] and 100% after 16 h [69]). However, the Ti-AlPO catalysts

Table 2
Catalytic activities of Ti-grafted AlPO and Ti-grafted SBA-15 catalysts for oxidation of cyclohexene.[a]

Catalyst	Selectivity in %				Total yield[b] in %	TON[c]	TOF[d] (h^{-1})
	Epoxide	Diol	Ene-ol	Ene-one			
Ti-AlPO	93	6	0	1	6.2	24	21
Ti-AlPOC	87	5	2	6	3.9	13	6.3
Ti-SBA15	>99	0	0	<1	16	30	17
Ti-SBA15C	>99	0	0	<1	13	25	14

[a] Reaction conditions: 25 mg catalyst, 9.88 inniol cyclohexene, 5.5 mmol TBHP? 5 niL acetonitrile, reaction temperature 65 °C, results obtained after 6 h of reaction.
[b] Total Yield = moles of cyclohexene oxide products relative to initial TBHP concentration.
[c] TON = mol epoxide mol^{-1} Ti.
[d] TOF – mol epoxide mol^{-1} Ti h^{-1} after 1 h.

reported here, in possessing surfaces containing associated, and possibly higher coordinate titanium species, are expected to exhibit a lower efficiency than catalysts with predominantly isolated, mononuclear, and 4-coordinate Ti centers. For example, Jarupatrakorn and coworkers reported single-site Ti-SBA15 catalysts with isolated titanium centers, which provide a very high TOF of 257 h^{-1}, using TBHP [10].

In an attempt to circumvent the tendency of $Ti(O^iPr)_4$ to condense on the surface and to promote the formation of isolated Ti catalytic sites, the amount of $Ti(O^iPr)_4$ used in the grafting process was decreased. Thus, calcined Ti-AlPO samples with Ti loadings of 0.89, 1.43, and 2.57 wt.%, corresponding to 0.23, 0.37, and 0.98 Ti/nm^{-2}, respectively, were prepared. For each sample, DRUV–vis spectroscopy measurements reveal the presence of both isolated Ti(IV) atoms in tetrahedral coordination (band at ca. 215 nm) and surface oligomeric titanium species (band at ca. 255 nm) (refer to Fig. A2). This indicates that the presence of isolated titanium centers is not enhanced at lower Ti content, and $Ti(O^iPr)_4$ still condenses on the surface to form oligomeric species. In addition, the shoulder corresponding to oligomeric species is more intense at lower loadings, which may indicate a more important contribution of oligomerized species. Thus, in term of catalytic performances, a decrease in efficiency is observed with decreased Ti loading, and lower Ti content corresponds to lower activity in term of TOFs (Fig. A3).

Additionally, it was observed that calcination has a deactivating effect on this catalyst (Table 2). It is reasonable to assume that the calcination process results in a higher amount of high-coordinate (and less active) titanium, and this is substantiated by DRUV–vis spectroscopy (*vide supra*). Indeed, the mobility of uncalcined titanium species could lead to oligomerization [70], and a relatively higher number of single-site tetrahedral Ti sites on the uncalcined materials is consistent with better catalytic properties.

In Table 3, the distribution of epoxidation products (cyclohexene epoxide and cyclohexan-1,2-diol) and allylic oxidation products (2-cyclohexen-1-ol and 2-cyclohexen-1-one) is depicted for Ti-AlPOC and Ti-SBA15C. Epoxidation seems to be greatly favored over allylic oxidation using silica as a grafting support for $Ti(O^iPr)_4$, as no allylic oxidation products were observed. On the other hand, Ti-AlPOC catalysts exhibit a selectivity of up to 39% for the formation of allylic products after 1 h, which then decreases by up to 8% after 6 h. A control experiment was conducted with pure mesoporous AlPO as an epoxidation catalyst with TBHP as oxidant (Table 3). After a reaction time of 1 h, the AlPO material exhibited a selectivity of 90% for the formation of the allylic products, with a low yield of 0.2%. With SBA-15, under the same experimental conditions, no cyclohexene oxidation products were observed over the same time period. This suggests that the AlPO surface in some way promotes the generation of radicals, since allylic oxidation is believed to proceed through a radical mechanism [71]. The presence of surface hydroxyl groups Al–OH and P–OH may play a role in the enhancement of this radical pathway. To test for this, a low concentration of a radical scavenger (4.5×10^{-4} M of 2,6-di-*tert*-butyl-4-methylphenol) was added to the reaction mixture containing AlPO and TBHP in acetonitrile. Under these conditions, the yield of allylic products drastically decreased. In a similar manner, the Ti-AlPOC catalyst was studied in the absence and presence of the same radical trap. Without the radical trap, the yield of allylic products was 1.1% and the selectivity for epoxidation was 61% after 1 h. With addition of the radical trap, the yield drastically decreased to 0.05% and the selectivity for epoxidation increased to 89%. This clearly suggests a Ti-mediated radical mechanism pathway, regardless of the intrinsic activity of the AlPO support. In addition, the absence of allylic products using Ti-SBA15 catalysts indicates that Ti centers on AlPO are in some way activated toward allylic oxidation. The presence of residual surface Al–OH and P–OH hydroxyl groups on Ti-AlPO – that are not present on Ti-SBA15 – may be responsible for this behavior.

Table 3
Distribution of non-radical and radical mechanism oxide products for the oxidation of cyclohexene over AlPO, Ti-grafted AlPO and Ti-grafted SBA-15 catalysts.

Catalyst	Time in h	% Non-radical mechanism[a]	% Radical mechanism[b]
AlPO	1	10	90
	6	9	91
Ti-AlPOC	1	61	39
	6	92	8
Ti-SBA15C	1	>99	<1
	6	>99	<1

[a] Mol [epoxide + diol]/mol [total oxide products] × 100.
[b] Mol [ene-ol + ene-one]/mol [total oxide products] × 100.

The influence of the peroxide oxidant has also been investigated. In metal-catalyzed epoxidations, the nature of the peroxide plays an important role in the selectivities and conversions in the epoxidation process. Thus, aqueous hydrogen peroxide (30 wt.% H_2O_2) was employed as an oxidant in acetonitrile at 65 °C. The Ti-AlPOC sample was found to exhibit a lower TON and a lower selectivity for epoxidation with H_2O_2 after 1 h, in comparison with the use of the organic peroxide TBHP (Table 4). This low activity is undoubtedly due to the presence of water, which is known to inhibit the epoxidation reaction [72]. To render the catalysts tolerant toward aqueous H_2O_2, the surface of Ti-AlPOC was modified with hydrophobic trimethylsilyl groups by treatment with an excess of $Me_3Si\text{-}NMe_2$ in hexane at room temperature, following the procedure described by Brutchey et al. [9]. The surface modification was confirmed by ^{13}C and ^{29}Si MAS NMR (refer to Fig. A4). The surface-modified catalyst, Me_{Cap}Ti-AlPO, was slightly more active for the oxidation of cyclohexene (TON of 2.3) than for that of the corresponding unmodified catalyst (TON of 0.9) using H_2O_2. The enhancement in catalytic activity after surface modification suggests that the hydrophobic surface slows water coordination to the surface-bound Ti(IV) sites, and/or increases the affinity of cyclohexene for the surface. In addition, the surface-modified

Table 4
Ti-AlPO-catalyzed oxidation of cyclohexene with TBHP and H_2O_2 at 65 °C at a reaction time of 1 h.

Catalyst	Oxidant	Selectivity in %				TOF
		Epoxide	Diol	Ene-ol	Ene-one	mol ep. mol^{-1} Ti h^{-1}
Ti-AlPOC	TBHP	61	0	8	31	6.33
	H_2O_2	12	39	14	35	0.91
Me_{Cap}Ti-AlPO	TBHP	67	0	10	23	1.61
	H_2O_2	21	32	13	34	2.31

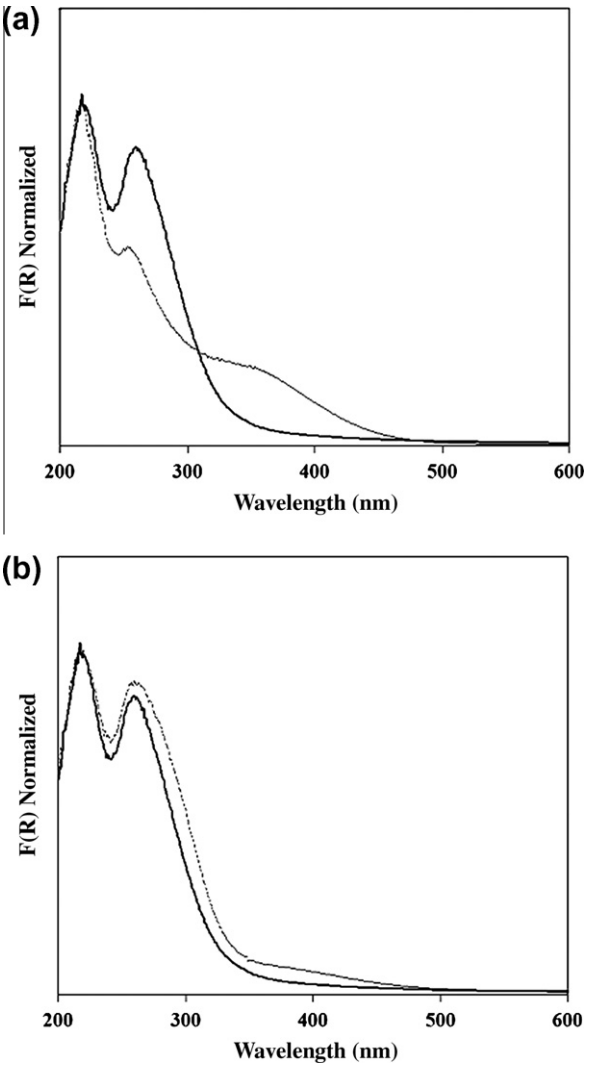

Fig. 9. DRUV–Vis spectra of Ti-AlPO calcined at 300 °C before (thick line) and after (thin line) exposure to (a) H_2O_2 and (b) TBHP.

catalyst was slightly more selective for epoxidation, as a result of a lower hydrolytic conversion of epoxide to cyclohexanediol. By using TBHP as an oxidant, with surface-modified catalyst, a lower TON for cyclohexene oxide was obtained. We suggest that this decrease in activity results from the greater steric bulk of the oxidant, which may hinder its access to the active sites. In addition, the selectivity for epoxidation was observed to be relatively unaffected by surface modification (61% and 67%, before and after surface modification, respectively).

For oxidation reactions mediated by titanium-containing catalysts, the nature of the intermediate resulting from activation of the oxidant (e.g., TBHP and H_2O_2) appears to be critical. To investigate the formation of such species, aqueous H_2O_2 and anhydrous TBHP were allowed to react with Ti-AlPOC for 3 h at 65 °C in acetonitrile. The samples turned strong yellow and pale orange when using H_2O_2 and TBHP, respectively, as evidence that Ti(IV)-peroxy species formed [73,74]. Fig. 9 shows DRUV–vis spectra of Ti-AlPOC before and after exposure to the oxidants. After exposure, the samples were rinsed thoroughly with acetonitrile and then dried under vacuum. A broad absorption from 300 to 480 nm with a maximum at 360 nm was observed after contact with H_2O_2, which is characteristic of a LMCT band for titanium-hydroperoxo (Ti–OOH) species [74,75]. Upon reaction with TBHP, the band is shifted to higher wavelengths, from 350 to 500 nm and centered around 390 nm, and is very weak as expected for the pale orange coloration of the sample. Note that the peak at 260 nm is slightly broader after adding TBHP, perhaps indicating a higher amount of high-coordination number Ti species. These results are in good agreement with those described for formation of 6-coordinate Ti(IV) with both η^1-OO^{t}Bu and η^2-OO^{t}Bu ligands, as suggested by Barker et al. [76] in the case of Ti-MCM41 and TBHP.

4. Conclusions

A mesoporous material with an AlPO structure containing grafted surface titanium species was synthesized and compared to a related sample prepared by grafting titanium in the same way to silica SBA-15. This comparison shows that there is not a significant influence of the nature of the support, AlPO vs. SBA-15, on the coordination environment of titanium ions. In both cases, grafting by Ti(O^{i}Pr)$_4$ yielded isolated 4-coordinate Ti(IV) centers and polymeric titanium species. The Ti-AlPO materials represent a new type of oxidation catalyst, as demonstrated in epoxidation studies with cyclohexene. The Ti-AlPO and Ti-SBA15 materials exhibit comparable activities and selectivities, which may be related to the similar natures of their active sites. In addition, the Ti-AlPO catalysts exhibit a higher tendency toward allylic oxidation, in comparison with similar Ti-SBA15 catalysts. This result potentially opens the way to exploitation of titanium-derived AlPO systems in allylic oxidations of interest. Future reports will describe additional aspects of the coordination chemistry of metals bound to mesoporous aluminophosphates and new catalytic transformations derived therefrom.

Acknowledgments

This work was supported by the Director, Office of Science, Office of Basic Energy Sciences of the US Department of Energy under Contract No. DE-AC02-05CH11231. L.R. acknowledges funding provided by the "Direction générale des Armements" (France, DGA). The authors are grateful to Dr. Chris Canlas for recording the solid-state NMR spectra. Parts of this research were carried out at ALS and SSRL funded by DOE, OBES. The SSRL SMB Program is supported by the DOE, Office of Biological and Environmental Research and by the NIH, National Center for Research Resources (NCRR).

Appendix A. Supplementary material

Supplementary data associated with this article can be found, in the online version, at doi:10.1016/j.jcat.2011.09.023.

References

[1] G. Clerici, in: M.G. Guisnet Jr., J. Barrault, C. Bouchoule, D. Duprez, G. Perot, C. Montassier (Eds.), Heterogeneous Catalysis and Fine Chemicals III, vol. 78, Elsevier, Amsterdam, 1993, p. 78.
[2] B. Notari, Adv. Catal. 41 (1996) 253.
[3] M.G. Clerici, G. Belussi, U. Romano, J. Catal. 129 (1991) 1.
[4] C.B. Khouw, C.B. Dartt, X. Li, M.E. Davis, ACS Symp. Ser. 523 (1993) 273.
[5] M.A. Camblor, A. Corma, A. Martinez, J. Perez Pariente, J. Chem. Soc., Chem. Commun. 8 (1992) 589.
[6] D.R.C. Huybrechts, Ph.L. Buskens, P.A. Jacobs, Stud. Surf. Sci. Catal. 72 (1992) 21.
[7] C.T. Kresge, M.E. Leonowicz, W.J. Roth, J.C. Vartuli, J.S. Beck, Nature 359 (1992) 710.
[8] J.C. van der Waal, M.S. Rigutto, H. van Bekkum, Appl. Catal. A – Gen. 167 (1998) 331.
[9] R.L. Brutchey, D.A. Ruddy, L.K. Andersen, T.D. Tilley, Langmuir 21 (2005) 9576.
[10] J. Jarupatrakorn, T.D. Tilley, J. Am. Chem. Soc. 124 (2002) 8380.
[11] S.T. Wilson, B.M. Lok, C.A. Messina, T.R. Cannan, E.M. Flanigen, J. Am. Chem. Soc. 104 (1982) 1146.
[12] T. Kimura, Micropor. Mesopor. Mater. 77 (2005) 97.
[13] M. Tiemann, M. Schulz, C. Jäger, M. Fröba, Chem. Mater. 13 (2001) 2885.
[14] D.Y. Zhao, Z.H. Luan, L. Kevan, Chem. Commun. 11 (1997) 1009.
[15] G. Lischke, B. Parlitz, U. Lohse, E. Schreier, R. Fricke, Appl. Catal. A – Gen. 166 (1998) 351.
[16] M.J. Haanepen, J.H.C. van Hoff, Appl. Catal. A – Gen. 152 (1997) 183.
[17] M. Hartmann, L. Kevan, Res. Chem. Intermediat. 28 (2002) 625.
[18] M. Stöcker, Micropor. Mesopor. Mater. 29 (1993) 3.
[19] N. Ulagappan, V. Krishnasamy, J. Chem. Soc., Chem. Commun. (1995) 373.
[20] M.H. Zahedi-Niaki, P.N. Joshi, S. Kaliaguine, Stud. Surf. Sci. Catal., vol. 105, Part A–C, Elsevier, Seoul, 1997, p. 1013.
[21] B.-Y. Hsu, S. Cheng, J.-M. Chen, J. Mol. Catal. A 149 (1999) 7.
[22] F.J. Luna, S.E. Ukawa, M. Wallau, U. Schuchardt, J. Mol. Catal. 117 (1997) 405.
[23] P. Selvam, S.K. Mohapatra, Micropor. Mesopor. Mater. 73 (2004) 137.
[24] S.K. Mohapatra, F. Hussain, P. Selvam, Catal. Commun. 4 (2003) 57.
[25] M.P. Kapoor, A. Raj, Appl. Catal. A – Gen. 203 (2000) 311.
[26] E. Gianotti, E.C. Oliveira, S. Coluccia, H.O. Pastore, L. Marchese, Inorg. Chim. Acta 349 (2003) 259.
[27] B.Z. Tian, X.Y. Liu, B. Tu, C.Z. Yu, J. Fan, L.M. Wang, S.H. Xie, G.D. Stucky, D.Y. Zhao, Nat. Mater. 2 (2003) 159.
[28] L.M. Wang, B.Z. Tian, J. Fan, X.Y. Liu, H.F. Yang, C.Z. Yu, B. Tu, D.Y. Zhao, Micropor. Mesopor. Mater. 67 (2004) 123.
[29] D. Zhao, Q. Huo, J. Feng, B.F. Chmelka, G.D. Stucky, J. Am. Chem. Soc. 120 (1998) 6024.
[30] R.F. Mortlock, A.T. Bell, C.J. Radke, J. Phys. Chem. 97 (1993) 767.
[31] J. Yu, R. Xu, J. Li, Solid State Sci. 2 (2000) 181.
[32] K.L. Fudjala, T.D. Tilley, J. Am. Chem. Soc. 123 (2001) 10133.
[33] M. Ritala, M. Leskelä, L. Niinistö, P. Haussalo, Chem. Mater. 5 (1993) 1174.
[34] F. Zhang, X. Carrier, J.-M. Krafft, Y. Yoshimura, J. Blanchard, New J. Chem. 34 (2010) 508–516.
[35] J. Chen, P.A. Wright, J.M. Thomas, S. Natarajan, L. Marchese, S.M. Bradley, G. Sankar, C.R.A. Catlow, J. Phys. Chem. 98 (1994) 10216.
[36] N.C. Masson, H.O. Pastore, Micropor. Mesopor. Mater. 44 (2001) 173.
[37] L. Marchese, T. Maschmeyer, E. Gianotti, S. Coluccia, J.M. Thomas, J. Phys. Chem. B 101 (1997) 8836.
[38] C.G. Barraclough, D.C. Bradley, J. Lewis, I.M. Thomas, J. Chem. Soc. (1961) 2601.
[39] H. Pfeifer, H. Ernst, Annu. Rep. NMR Spectrosc. 28 (1994) 91.
[40] M.H. Zahedi-Niaki, S.M. Javaid Zaidi, S. Kaliaguine, Micropor. Mesopor. Mater. 32 (1999) 251.
[41] J. Klinowski, Chem. Rev. 91 (1991) 1459.
[42] M. Hunger, Catal. Rev. 39 (1997) 345.
[43] T.-H. Chen, B.H. Wouters, P.J. Grobet, J. Phys. Chem. B 103 (1999) 6179.
[44] V.M. Mastikhin, I.L. Moudrakovski, V.P. Shmatchkova, N.S. Kosarenko, Chem. Phys. Lett. 139 (1987) 93.
[45] S.D. Mikhailenko, J. Zaidi, S. Kaliaguine, J. Chem. Soc. Faraday Trans. 94 (1998) 1613.
[46] M. Stöcker, in: H. Chon, S.I. Woo, S.-E. Park (Eds.), Studies in Surface Science and Catalysis, vol. 102, Elsevier, Amsterdam, 1996, p. 141.
[47] T. Blasco, A. Corma, M.T. Navarro, J. Perez Pariente, J. Catal. 156 (1995) 65.
[48] S. Klein, B.M. Weckhuysen, J.A. Martens, W.F. Majer, P.A. Jacobs, J. Catal. 163 (1999) 489.
[49] J. Klaas, G. Schultz-Ekloff, N.I. Jaeger, J. Phys. Chem. B 101 (1997) 1305.
[50] A.O. Bouh, G.L. Rice, S. Scott, J. Am. Chem. Soc. 121 (1999) 7201.
[51] M.C. Capel-Sanchez, G. Blanco-Brieva, J.M. Campos-Martin, M.P. de Frutos, W. Wen, J.A. Rodriguez, J.L.G. Fierro, Langmuir 25 (2009) 7148.
[52] E. Gianotti, A. Frache, S. Coluccia, J.M. Thomas, T. Maschmeyer, L. Marchese, J. Mol. Catal. A – Chem. 204–205 (2003) 483.
[53] C. Blandy, J.-L. Pellegatta, R. Choukroun, B. Gilot, R. Guiraud, Can. J. Chem. 71 (1993) 34.
[54] R. Ghosh, M. Nethaji, A.G. Samuelson, J. Organomet. Chem. 690 (2005) 1282.
[55] R.B. Greegor, F.W. Lytle, D.R. Sandstrom, J. Wong, P. Schultz, J. Non-Cryst. Solids 55 (1983) 27.
[56] G.A. Waychunas, Am. Mineralog. 72 (1987) 89.
[57] F. Farges, G.E. Brown Jr., J. Rehr, J. Phys. Rev. B 56 (1997) 1809.
[58] Q. Yuan, A. Hagen, F. Roessner, Appl. Catal. A – Gen. 303 (2006) 81.
[59] A. Zhang, Z. Li, Y. Shen, Y. Zhu, Appl. Surf. Sci. 254 (2008) 6298.
[60] X. Gao, S.R. Bare, J.L.G. Fierro, M.A. Banares, I.E. Wachs, J. Phys. Chem. 102 (1998) 5653.
[61] O.A. Anunziata, A.R. Beltramone, M.L. Martinez, L.J. Giovanetti, F.G. Requejo, E. Lede, Appl. Catal. A – Gen. 397 (2011) 22.
[62] K.K. Wu, I.D. Brown, Acta Crystallogr. Sect. B 29 (1973) 2009.
[63] P.B. Moore, S.J. Louisnathan, Z. Kristallogr. 130 (1969) 438.
[64] E. Canillo, F. Mazzi, G. Rossi, Acta Crystallogr. 21 (1966) 200.
[65] C. Pan, S. Yuan, W. Zhang, Appl. Catal. A – Gen. 312 (2006) 186.
[66] M.H. Zahedi-Niaki, M.P. Kapoor, S. Kaliaguine, J. Catal. 177 (1998) 231.
[67] A. Bhaumik, S. Inagaki, J. Am. Chem. Soc. 123 (2001) 691.
[68] J.M. Fraile, J.I. Garcia, J.A. Moyoral, E. Vispe, D.R. Brown, M. Naderi, Chem. Commun. (2001) 1510.
[69] S. Sensarma, A.O. Bouh, S.L. Scott, H. Alper, J. Mol. Catal. A: Chem. 203 (2003) 145.
[70] L. Marchese, E. Gianotti, V. Dellarocca, T. Maschmeyer, F. Rey, S. Coluccia, J.M. Thomas, Phys. Chem. Chem. Phys. 1 (1999) 585.
[71] J.M. Fraile, J.I. Garcia, J.A. Mayoral, E. Vispe, J. Catal. 204 (2001) 146.
[72] R.A. Sheldon, J. Mol. Catal. 7 (1980) 107.
[73] E. Gianotti, C. Bisio, L. Marchese, M. Guidotti, N. Ravasio, R. Psaro, S. Coluccia, J. Phys. Chem. C 111 (2007) 5083.
[74] W. Lin, H. Frei, J. Am. Chem. Soc. 124 (2002) 9292.
[75] S. Bordiga, A. Damin, F. Bonino, G. Ricchiardi, C. Lamberti, A. Zecchina, Angew. Chem. Int. Ed. 41 (2002) 4734.
[76] C.M. Barker, D. Gleeson, N. Kaltsoyannis, C.R.A. Catlow, G. Sankar, J.M. Thomas, Phys. Chem. Chem. Phys. 4 (2002) 1228.